The one-carbon carrier methylofuran from Methylobacterium extorquens AM1 contains a large number of alpha- and gamma-linked glutamic acid residues

Jethro L. Hemmann, Olivier Saurel, Andrea M. Ochsner, Barbara K. Stodden, Patrick Kiefer, Alain Milon, Julia A. Vorholt

THE JOURNAL OF BIOLOGICAL CHEMISTRY VOL. 291, NO. 17, pp. 9042–9051, April 22, 2016

The One-carbon Carrier Methylofuran from *Methylobacterium extorquens* AM1 Contains a Large Number of α- and γ-Linked Glutamic Acid Residues*

Received for publication, January 8, 2016, and in revised form, February 17, 2016 Published, JBC Papers in Press, February 19, 2016, DOI 10.1074/jbc.M116.714741

Jethro L. Hemmann[‡], Olivier Saurel[§], Andrea M. Ochsner[‡], Barbara K. Stodden[¶], Patrick Kiefer[‡], Alain Milon[§], and Julia A. Vorholt[‡1]

From the [‡]Institute of Microbiology, ETH Zurich, Vladimir-Prelog-Weg 4, 8093 Zurich, Switzerland, [§]Institute of Pharmacology and Structural Biology, CNRS and Université de Toulouse-Paul Sabatier, 31077 Toulouse, France, and [¶]Laboratoire des Interactions Plantes Microorganismes, INRA/CNRS 441-2594, Castanet Tolosan, France

Methylobacterium extorquens **AM1 uses dedicated cofactors for one-carbon unit conversion. Based on the sequence identities of enzymes and activity determinations, a methanofuran analog was proposed to be involved in formaldehyde oxidation in Alphaproteobacteria. Here, we report the structure of the cofactor, which we termed methylofuran. Using an *in vitro* enzyme assay and LC-MS, methylofuran was identified in cell extracts and further purified. From the exact mass and MS-MS fragmentation pattern, the structure of the cofactor was determined to consist of a polyglutamic acid side chain linked to a core structure similar to the one present in archaeal methanofuran variants. NMR analyses showed that the core structure contains a furan ring. However, instead of the tyramine moiety that is present in methanofuran cofactors, a tyrosine residue is present in methylofuran, which was further confirmed by MS through the incorporation of a ^{13}C-labeled precursor. Methylofuran was present as a mixture of different species with varying numbers of glutamic acid residues in the side chain ranging from 12 to 24. Notably, the glutamic acid residues were not solely γ-linked, as is the case for all known methanofurans, but were identified by NMR as a mixture of α- and γ-linked amino acids. Considering the unusual peptide chain, the elucidation of the structure presented here sets the basis for further research on this cofactor, which is probably the largest cofactor known so far.**

First termed carbon dioxide reduction factor (1), methanofuran (MFR)[2] was discovered in 1983, and its structure was identified after purification from cell extracts of *Methanothermobacter thermautotrophicus* (2). MFR, tetrahydromethanopterin (H_4MPT) (3, 4), and coenzyme M (5) are cofactors that serve as the carrier molecule for one-carbon units at the oxidation states of formate, formaldehyde, and methanol, respectively, and were originally thought to be unique to the group of strict anaerobic methanogenic archaea (6). The importance of "archaeal" cofactors for one-carbon unit conversion was later extended to aerobic bacteria with the discovery of "methanogenic" enzymes in the methylotrophic model bacterium *Methylobacterium extorquens* AM1. This bacterium harbors enzymes with sequence identity to those from methanogens, and the enzymes were active with the cofactors MFR and H_4MPT purified from *M. thermautotrophicus* (7). Although H_4MPT was identified as dephospho-H_4MPT (7), the identity of the assumed MFR analog remained unknown in *M. extorquens* AM1 and other methylotrophic bacteria (8–10).

In *M. extorquens* AM1, the one-carbon carrier coenzymes are involved in the oxidation of formaldehyde, which is generated from methanol (or methylamine) (11) (Fig. 1). After the enzyme-assisted binding of formaldehyde to H_4MPT (12), dehydrogenation (13), and hydrolysis to formyl-H_4MPT (8), the one-carbon unit is transferred to the MFR analog as shown with purified enzyme (14). Notably, and in contrast to the enzymes from methanogenic archaea, the formyl group is subsequently hydrolyzed and released as free formate by the formyltransferase-hydrolase complex (Fhc) (15). The oxidation pathway is then completed by formate dehydrogenases (16), or alternatively, formate is fed into the serine cycle (17, 18) for biomass formation via tetrahydrofolate (19).

To date, five different variants of the MFR cofactor, labeled MFR-a to MFR-e, have been identified and structurally characterized in different methanogenic archaea (2, 20–22). These MFR variants all have a common core structure consisting of an APMF-moiety (4-[[4-(2-aminoethyl)phenoxy]-methyl]-2-furanmethanamine) linked to at least two γ-glutamic acid residues (Fig. 2*A*, example of MFR-a). The APMF core structure consists of a furan derivative attached to a tyramine residue. The different MFR variants show remarkable chemical variability, as different moieties, such as the hexanetetracarboxylic acid group in MFR-a or additional glutamic acid residues (MFR-b, MFR-d, MFR-e), can be attached to the side chain of the AMPF-γ-Glu_2 structure. Modifications are also possible in the center of the polyglutamic acid side chain, as in the case of MFR-e, where an unusual spacer has been identified (22). In MFR-d and MFR-e, the number of glutamic acid residues is variable, ranging from 7 to12 and from 5 to 8, respectively (22). Some work has also been dedicated to the MFR biosynthesis, and six

* This work was supported by ETH Zurich, the Centre National de la Recherche Scientifique, and the Max-Planck-Society. The authors declare that they have no conflicts of interest with the contents of this article.
[1] To whom correspondence should be addressed. Tel.: 41-44-632-55-24; Fax: 41-44-633-13-07; E-mail: jvorholt@ethz.ch.
[2] The abbreviations used are: MFR, methanofuran; H_4MPT, tetrahydromethanopterin; Fhc, formyltransferase/hydrolase complex; cww, cell wet weight; cdw, cell dry weight; TOCSY, total correlation spectroscopy; APMF, 4-[[4-(2-aminoethyl)phenoxy]-methyl]-2-furanmethanamine; DSS, 4,4-dimethyl-4-silapentane-1-sulfonic acid; DQF, double quantum filtered.

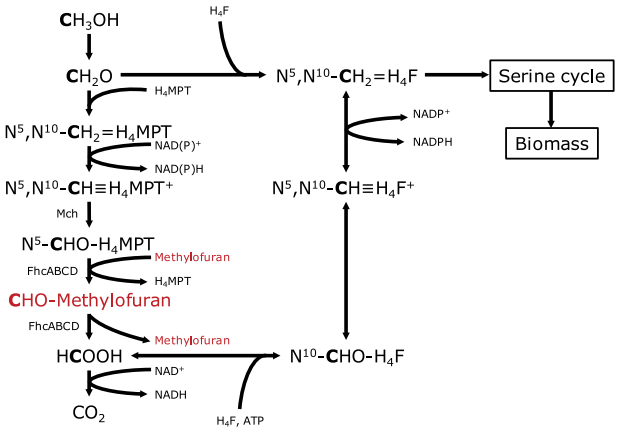

FIGURE 1. **Pathway for C_1 assimilation in *M. extorquens* AM1.** Metabolic pathway for the assimilation of C_1-substrates involving the cofactors H_4MPT, tetrahydrofolate (H_4F) and methylofuran, which is identified in this study. CH_2═, CH≡, and CHO—, attached methylene, methenyl, and formyl group respectively.

enzymes (MfnA-F) have been identified in *Methanocaldococcus jannaschii* so far (23–26).

The essential role of enzymes that depend on the putative MFR analog in *M. extorquens* AM1 and other methylotrophs prompted us to identify the cofactor. We structurally characterize the cofactor from the model bacterium using high resolution MS and NMR and propose the name "methylofuran" to take into account that it shows features not found in known MFR variants from methanogens so far.

Experimental Procedures

Chemicals—Formyl-MFR-a was purified from *Methanothermobacter marburgensis* as described (27) and was a gift from R.K. Thauer (MPI Marburg, Germany).

Custom-synthesized polyglutamic acid peptides of the sequences $E_{10}Y$ and $(\gamma E)_{20}Y$ (crude purity) were obtained from Thermo Fisher Scientific (Ulm, Germany). The $(\gamma E)_{20}Y$ peptide contained γ-linkages between the glutamic acids, whereas the $E_{10}Y$ peptide was α-linked. 1-^{13}C-Labeled L-tyrosine and U-$^{13}C_9$,^{15}N-labeled L-tyrosine (purity 99%) were both ordered from ReseaChem (Burgdorf, Switzerland).

Large Scale Cultivation of M. extorquens AM1—*M. extorquens* AM1 was grown in minimal medium containing 123 mM (0.5% v/v) methanol as the carbon source, mineral salts (30.3 mM NH_4Cl, 1.9 mM $MgSO_4$, 21 mM $(NH_4)_2SO_4$), buffer (13.8 mM K_2HPO_4, 6.9 mM NaH_2PO_4), trace elements (37.6 μM $ZnSO_4$, 30.3 μM $CoCl_2$, 12.2 μM $MnCl_2$, 38.8 μM H_3BO_3, 4.0 μM Na_2MoO_4, 2.9 μM $CuSO_4$, 191.9 μM $CaCl_2$), and iron (322.4 μM Na_2EDTA, 86.3 μM $FeSO_4$). The pH was kept constant at 7.0 through the addition of 2 M ammonia, the temperature was set to 28 °C, and the aeration and stirring rate were set to 2 liters/min and 1500 rpm, respectively. For the initial identification of methylofuran, a first batch of *M. extorquens* AM1 cell material, referred to as batch A, was produced by growing the cells in a 300 liters fermenter. The final yield was 1.2 kg cww.

A second batch of biomass, referred to as batch B, was prepared in a 3.6 liters bioreactor (Infors) filled with 1.4 liters of minimal medium as fed-batch culture. The methanol feed was controlled using a control sequence that added 6 ml of methanol to the medium as soon as the available methanol was used up by the cells, as detected by the rise in the dissolved oxygen level. After the culture had reached an A_{600} of 50–70, ~1.3 liters of the culture was harvested by centrifugation, leaving the rest of the culture as inoculum for the next batch. The next culture was then immediately started through the addition of 1 liter of fresh medium. This procedure was repeated 14 times, yielding in total ~340 g cdw (assuming 300 μg/ml cdw per A_{600} unit). Cell pellets were frozen at −20 °C until further processing.

Extraction of Methylofuran—Cell material from batch A was split into 300 g cww portions. Every portion was suspended in 250 ml of 10 mM potassium phosphate buffer at pH 7 and processed independently. Cells were lysed through the addition of 69 ml of 5% hexadecyltrimethylammonium bromide solution and incubated at 30 °C for 10 min. Cell debris was removed by centrifugation. The resulting pellet was resuspended in 100 ml of 10 mM potassium phosphate buffer at pH 7 and centrifuged again. The supernatants from both steps were combined. To remove proteins, the cell extract was incubated at 75 °C for 10 min. After centrifugation, the soluble fraction was ready for purification.

Cell material from batch B was divided into six portions of ~50 g cdw each. Each portion was resuspended in 2.5 ml of water and 3 ml of methanol per g cdw and processed independently. The resuspended cell material was lysed and extracted by boiling the cells in closed bottles in a water bath at 100 °C for 10 min. After cooling on ice, the suspension was centrifuged, and the resulting pellet was re-extracted twice at 100 °C using the same amounts of water and methanol as before. The extracts were combined and concentrated to about half their volume in a rotary evaporator, thereby removing most of the methanol. After freeze-drying the extracts, the dried powder was dissolved in 50 ml of 20 mM ammonium bicarbonate buffer, and the pH was adjusted to 8.4. After ultracentrifugation at 47,000 g for 1 h, the extracts were used for purification.

Purification of Methylofuran—For the purification of the cell extracts from batch A, an enzymatic assay was used for the identification of the fractions containing methylofuran. This assay has been previously described as an alternative assay for the determination of formyltransferase activity (14). Briefly, it involves the enzymes Fhc and methenyl-H_4MPT cyclohydrolase (Mch). Methenyl-H_4MPT cyclohydrolase catalyzes the formation of formyl-H_4MPT from methenyl-H_4MPT, whereas Fhc catalyzes the transfer of the formyl group from formyl-H_4MPT to methylofuran (Fig. 1). The generation of formyl-MFR was indirectly observed through the spontaneous reduction of cytochrome *c* by released H_4MPT, as monitored by the increase in absorbance at 550 nm. The reaction was started by the addition of fractions containing methylofuran.

Cell extracts from batch A were first purified on a Source 15Q column (16 × 100 mm, Amersham Biosciences), equilibrated with 10 mM acetic acid at pH 5. Elution was performed using the following gradient: 30 ml of 0 M NaCl, 10 ml of 0–0.2 M NaCl, 60 ml of 0.2 M NaCl, 150 ml of 0.2–1 M NaCl. Methylofuran was identified in the fraction eluting at 0.4 M NaCl. A second step of purification was performed using a hydroxyapatite column (16 × 100 mm, Bio-Rad) equilibrated with 10 mM

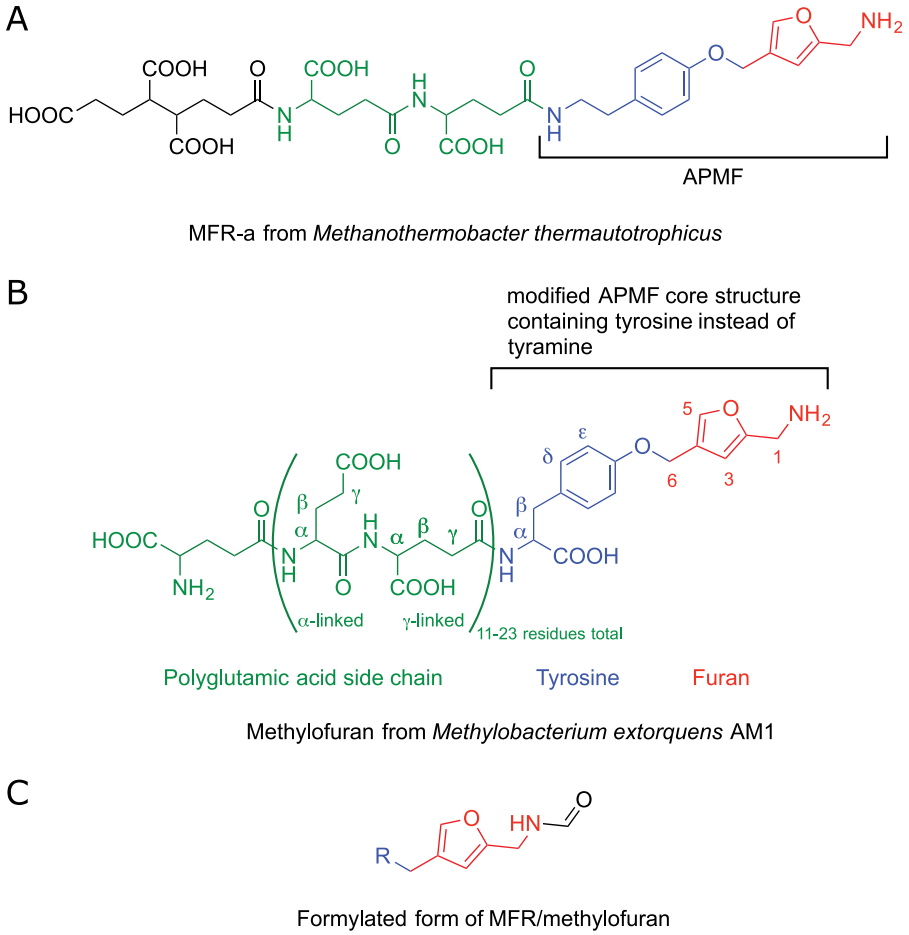

FIGURE 2. **Comparison of the structure of MFR-a with methylofuran found in *M. extorquens* AM1.** *A*, chemical structure of the MFR-a cofactor found in *Methanothermobacter thermautotrophicus* (2). *B*, chemical structure of methylofuran, as proposed in this work. Note that the glutamic acids, although shown here with alternating γ/α-linkages, may contain other arrangements of α/γ-linkages. *C*, structure indicating the position of the formyl group (one-carbon unit) present in the formylated form of MFR/methylofuran.

potassium phosphate at pH 7. The following gradient was applied: 55 ml of 10–35 mM potassium phosphate, 5 ml of 35–100 mM potassium phosphate, 50 ml of 100 mM potassium phosphate. Methylofuran eluted at 28 mM potassium phosphate. The sample was further purified using a 6-ml Resource Q column (Amersham Biosciences). A pH gradient with 10 mM acetic acid solution between pH 5 and 3 was applied, but methylofuran could not be eluted under these conditions. A linear gradient of 20 ml of 0–0.4 M NaCl in 10 mM acetic acid at pH 5 was, therefore, used for elution. For further purification by HPLC, desalting was required. The sample was, therefore, loaded on a Superdex Peptide HR 10/30 column (Amersham Biosciences) and separated from salts using 30 ml of water. HPLC purification was performed on a Discovery HS F5 column (4.6 × 150 mm, Supelco) using 10 mM acetic acid, pH 3.2, as solvent A and acetonitrile for solvent B. Elution was performed at 0.7 ml/min with the following gradient: 3.5 ml of 0% B, 10.5 ml of 0–10% B, 3.5 ml of 10% B, 10.5 ml of 10–30% B. The retention time for methylofuran was 32 min. For further purification, anion exchange on a Mono Q HR 5/5 column (Amersham Biosciences) was performed using a linear gradient of 20 ml of 0–0.8 M NaCl in 10 mM potassium phosphate at pH 7. Methylofuran eluted at 0.6 M NaCl. Finally, an extraction using tetrahydrofuran (THF) was performed. The lyophilized sample was dissolved in 7 ml of THF and centrifuged. Methylofuran could be detected in the solid phase and was redissolved in water. For NMR measurements, the sample was again desalted using the Superdex Peptide column as described above and freeze-dried.

Cell extracts from batch B were purified according to a simplified protocol involving only anion-exchange chromatography. In one run 10 ml of the cell extract (corresponding to ~10 g cdw) of one portion were loaded on a 15-ml Mono Q column (GE Healthcare). Elution was performed using a linear gradient from 1% to 100% of 2 M ammonium bicarbonate at pH 8.4 within 144 ml. The flow rate was set to 4 ml/min, and 14-ml fractions were collected. The fractions containing methylofuran were identified using LC-MS at ~1.2 M ammonium bicarbonate. They were pooled and concentrated to half their volume using a rotary evaporator, thereby also removing most of the ammonium bicarbonate. Because methylofuran eluted within a rather broad peak of other compounds and the loading capacity of the column was likely exceeded, the purified sample was run a second time through the same column. For this second purification, 2.5 ml of the sample was loaded per run, and 7-ml fractions were collected. Fractions containing methylofuran were pooled and freeze-dried for NMR measurements.

Cultivation of M. extorquens AM1 in Flasks and Extraction of Methylofuran for LC-MS—For the LC-MS analysis, only small amounts of methylofuran were required, and *M. extorquens* AM1 was cultivated in baffled flasks for this purpose. *M. extorquens* AM1 cells were grown in minimal medium containing mineral salts (30.3 mM NH_4Cl, 0.81 mM $MgSO_4$), buffer (13.8 mM K_2HPO_4, 6.9 mM NaH_2PO_4), trace elements (15.7 μM $ZnSO_4$, 12.6 μM $CoCl_2$, 5.09 $MnCl_2$, 16.2 μM H_3BO_3, 1.7 μM Na_2MoO_4, 1.2 μM $CuSO_4$, 20.4 μM $CaCl_2$), iron (40.3 μM Na_2EDTA, 10.8 μM $FeSO_4$), and 123 mM (0.5% v/v) methanol as a carbon source. For growth on succinate, the buffer was replaced by 9.13 mM K_2HPO_4 and 11.54 mM NaH_2PO_4, and 30.83 mM succinate was used as a carbon source. A preculture (20 ml), inoculated from glycerol stock, was used for the inoculation of a main culture (100–200 ml) to an A_{600} of ~0.05. All cultures were grown at 28 °C while shaking at 180 min^{-1}. After the culture reached an A_{600} of ~2–3, the cells were harvested by centrifugation.

Extraction of methylofuran was performed twice, similarly to as described above, through the addition of 1 ml of water and 1.2 ml of methanol to the cell pellet and the boiling of the suspension at 100 °C for 5 min. The extract was concentrated in a vacuum concentrator to ~1.4 ml and filtered through a 10-kDa centrifugal filter unit (Amicon Ultra-4, Merck Millipore). The filtered extract was then purified using a 2-ml Mono Q column (GE Healthcare). A 24-ml linear gradient from 1 to 100% of 2 M ammonium bicarbonate at pH 8.2 was applied for elution. The flow rate was set to 1 ml/min, and 1 ml fractions were collected. The fractions containing methylofuran were identified by LC-MS.

NMR Measurements—The dried samples prepared from batch A and batch B were dissolved in 500 μl of D_2O for NMR experiments performed at 298 K.

For the sample from batch A, NMR spectra were recorded with an Avance DMX500 spectrometer (Bruker Biospin) operating at 500.13 MHz. A one-dimensional spectrum was acquired with 20,486 scans into 16k data points across a spectral width of 7000.2 Hz with a relaxation delay of 1.17 s, and solvent suppression was achieved using a double echo Watergate scheme (*i.e.* W5) (28). ^1H,^1H COSY-DQF (29) and TOCSY (30) spectra were acquired with 128 scans into 2000 and 512 data points (in direct and indirect dimensions, respectively) across a spectral width of 5482 Hz using a relaxation delay of 1 s. The TOCSY mixing time was set to 70 ms using a MLEV-17 scheme.

Concerning the sample from batch B, NMR spectra were recorded with an Avance III HD spectrometer (Bruker Biospin) operating at 600.13 MHz and equipped with a TCI cryoprobe. A one-dimensional spectrum was acquired with 256 scans into 28,000 data points across a spectral width of 7211.5 Hz with a relaxation delay of 1 s. ^1H,^1H COSY-DQF and NOESY spectra were acquired into 8000 and 512 data points (in direct and indirect dimensions, respectively) across a spectral width of 7500 Hz with a relaxation delay of 1 s. The NOESY mixing time was set to 800 ms. COSY-DQF and NOESY spectra were recorded with 32 and 64 scans, respectively. The NMR data were processed using Topspin 3.2 software (Bruker Biospin). Chemical shifts were referenced with respect to 4,4-dimethyl-4-silapentane-1-sulfonic acid (DSS).

LC-MS Measurements—LC-MS measurements of samples from batch B were performed on an LTQ Orbitrap XL mass spectrometer (Thermo Fischer Scientific) coupled to a nano-2D Ultra LC system (Eksigent Technologies Inc.). For chromatographic separation, ion-pair reversed-phase HPLC using a C18 column (Dr. Maisch, Reprosil-Gold 120 C18 3 μm, 0.1 × 105 mm) was applied, as described previously (31). Solvent A was 1.7 mM tributylamine reagent in 1.5 mM acetic acid, pH-adjusted to pH 9.0 with ammonia, and solvent B was methanol. LC separation was performed at a flow rate of 400 nl min^{-1}, applying the following gradient of B: 0 min, 3%; 30 min, 90%; 35 min, 90%; 36 min, 3%; 45 min, 3%. Before analysis, samples were diluted 1:10 with solvent A, and 1 μl was injected. Samples were measured in negative FTMS mode at a unit resolution of 60,000 (at 400 m/z), applying nano-electrospray ionization with a spray voltage of −1.9 kV. Further source settings were a capillary temperature of 150 °C, capillary voltage of −10 V, and tube lens voltage of −100 V. The analysis of MS level two (MS-MS) was carried out on a Q Exactive Plus instrument (Thermo Fisher Scientific) coupled to an EASY-nLC 1000 (Thermo Fisher Scientific), applying an identical LC separation. For ionization, the spray voltage was set to −2.5 kV, and a capillary temperature of 250 °C was used. Fragmentation occurred in parallel reaction monitoring (PRM) mode with an isolation window of 2 Da, a collision energy of 30 eV, and a resolution of 35,000. LC-MS data analysis was performed using Xcalibur (Thermo Fisher Scientific) and the emzed framework (32).

Calculation of the Distribution of the Number of Glutamic Acid Residues in Methylofuran—The distribution of the number of glutamic acid residues of methylofuran was calculated by filtering the LC-MS data to generate mass traces with 7 ppm tolerance for all methylofuran species with 12–24 glutamic acid residues and considering charge states with $2 \leq z \leq 9$ and natural isotopologues with up to four [^{13}C]carbon atoms. The mass traces were integrated (trapezoid integration) over the elution time-window and normalized to produce the distribution. The analysis was implemented using emzed (32).

In Vivo ^{13}C-Labeling of the Tyrosine Moiety—For the incorporation of labeled tyrosine, *M. extorquens* AM1 cells were grown in flasks containing methanol minimal medium, as described above. For 1-^{13}C labeling, the preculture was grown in unlabeled medium and used for the inoculation of the main culture supplemented with 0.5 mM labeled tyrosine. For U-$^{13}C_9$,^{15}N labeling, the preculture and the main culture were both grown in medium containing 0.5 mM labeled tyrosine. After the 1-^{13}C and U-$^{13}C_9$,^{15}N cultures had reached an A_{600} of 2.3 and 3.8, respectively, they were harvested by centrifugation, extracted, and purified as described above. The fractions containing methylofuran were measured by LC-MS for the analysis of the labeling pattern.

Results

Identification of Methylofuran and Characterization by NMR—The discovery of a formyltransferase-hydrolase complex (FhcABCD) in *M. extorquens* AM1 (14, 15) and its activity with MFR from *M. marburgensis* suggested the presence of an MFR analog in the aerobic methylotroph. We, therefore, used an enzymatic assay we developed earlier (14) to monitor the

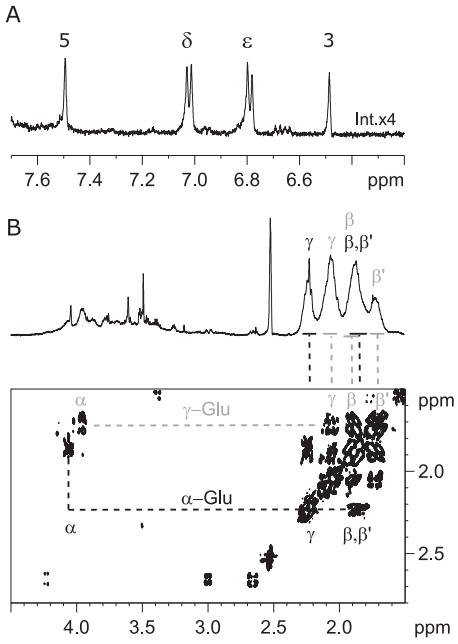

FIGURE 3. **^{1}H NMR spectra of methylofuran.** Peaks are annotated according to Fig. 2*B*. Spectra were recorded at 298 K in D_2O and calibrated with respect to 4,4-dimethyl-4-silapentane-1-sulfonic acid (DSS). *A*, part of the one-dimensional ^{1}H spectrum showing the aromatic resonances of the APMF-like moiety of the methylofuran. *B*, part of the ^{1}H,^{1}H COSY spectrum showing the α, β, and γ protons of the glutamic acid residues in the side chain. The two distinct spin systems correspond to glutamic acid residues with either α- or γ-linkages between the residues in the side chain.

transfer of the formyl group and to test for the presence of the methanofuran analog from the methylotroph in fractions obtained from consecutive preparative LC separation steps (see "Experimental Procedures"). Purified active fractions were measured by ^{1}H NMR for structural characterization. In the aromatic region of the one-dimensional spectrum, two doublets beside two singlets were observed (Fig. 3*A*), a pattern that is characteristic of the NMR signature of the APMF core structure of the methanofuran cofactors described previously (2, 15, 20, 22). The two singlets at 7.49 ppm (1H, s) and 6.49 ppm (1H, s) corresponded to the protons annotated with 5 and 3, respectively, on the furan ring in Fig. 2*B*, whereas the doublets at 7.01 ppm (2H, d) and 6.78 ppm (2H, d) are characteristic of the para-disubstituted aromatic cycle of the tyramine moiety of MFRs and were assigned to protons δ and ϵ, respectively. The spectrum was similar to those reported for the furan moiety and the tyramine aromatic ring in other MFRs, thereby confirming the presence of these two structures (Fig. 2*B*).

Furthermore, four broad resonances centered at 2.20 ppm, 2.00 ppm, 1.85 ppm, and 1.70 ppm were observed, a region of the spectrum corresponding to the side chain of the glutamic acid residues (Fig. 3*B*). The TOCSY and COSY spectra clearly revealed two distinct spin systems for the glutamic acid protons that corresponded to the presence of both α- and γ-linked glutamic acids in the side chain. The spin system characterized by the H_α at lower field (*i.e.* H_α 4.07 ppm, $H_{\beta,\beta'}$ 1.85 ppm, and H_γ 2.14 ppm) corresponded to α-linked residues, whereas the spin system with the H_α at higher field (*i.e.* H_α 3.96 ppm, H_β 1.89 ppm, $H_{\beta'}$ 1.72 ppm, and H_γ 2.06 ppm) was assigned to γ-linked residues (33). By integration, it was estimated that 65 ± 10% of the glutamic acid residues would be γ-linked and 35 ± 10% α-linked. Based on the TOCSY and NOESY spectra, a detailed description of the polyglutamic acid moiety (*e.g.* sequential assignment) was not possible, but the broadness and the integration strongly suggested a higher number of glutamic acid residues compared with known MFRs (Fig. 2*B*).

TABLE 1
List of the identified peaks in the negative-ion LC-MS mass spectra of methylofuran
Only a single charge state for each species is shown, although other charge states were also detected. The monoisotopic molecular mass was calculated from the measured *m*/*z*.

No. Glu	*z*	Measured *m*/*z*	Calculated *m*/*z*	Difference	Molecular mass	Retention time
				ppm	*Da*	*min*
12	2	918.3080	918.3116	3.9	1838.6306	19.50
13	2	982.8317	982.8329	1.2	1967.6780	19.58
14	2	1047.3514	1047.3542	2.7	2096.7174	19.70
15	2	1111.8716	1111.8755	3.5	2225.7578	19.79
16	3	783.9282	783.9288	0.8	2354.8065	19.85
17	3	826.9418	826.9430	1.5	2483.8473	19.95
18	3	869.9547	869.9572	2.9	2612.8860	20.04
19	3	912.9691	912.9714	2.5	2741.9292	20.14
20	3	955.9833	955.9856	2.4	2870.9718	20.20
21	3	998.9977	998.9998	2.1	3000.0150	20.27
22	3	1042.0127	1042.0140	1.2	3129.0600	20.37
23	3	1085.0263	1085.0282	1.8	3258.1008	20.44
24	3	1128.0414	1128.0424	0.9	3387.1461	20.50

Identification of the Molecular Formula of Methylofuran and Identity of Its Side Chain—The above described samples used for NMR were also analyzed by MALDI-MS, which indicated that methylofuran was not a single species but rather contained a varying number of glutamic acid residues in its side chain, roughly distributed between 10 and 20 residues (data not shown). For further characterization of methylofuran, a high resolution mass spectrometry (HR-MS) method was developed. As a chemically similar standard to the expected MFR analog, two custom-synthesized peptides containing 10 or 20 glutamic acid residues linked to a tyrosine ($E_{10}Y$ and $(\gamma E)_{20}Y$) were used for the development and optimization of the LC-MS method. In the $(\gamma E)_{20}Y$ peptide, the glutamic acid residues were exclusively γ-linked.

In a first trial, the HPLC separation of the peptides on a C18 reversed-phase column was attempted under acidic conditions (0.1% formic acid), a method that was successfully applied for the identification of MFR-d containing up to 12 glutamic acid residues (22). Using this method, however, only the peptide with 10 residues was retained on the column, whereas no retention of the peptide with 20 residues was observed, which could be explained by its much higher acidity. As an alternative, nano ion-pair reversed-phase HPLC using tributylamine as the ion pairing reagent at basic pH was applied, a method particularly suited for polar compounds (31). Both peptides showed good retention using this method and could be detected by MS in the negative-ion mode. All further measurements were, therefore, performed using nano-ion-pair reversed-phase LC-MS.

The measurement of purified *M. extorquens* AM1 cell extract showed a range of peaks, each separated by the mass of a glutamic acid residue (129.0426 Da). These peaks corresponded to different species of methylofuran with varying number of glutamic acid residues in their side chain (Table 1). The different species of methylofuran eluted from the column

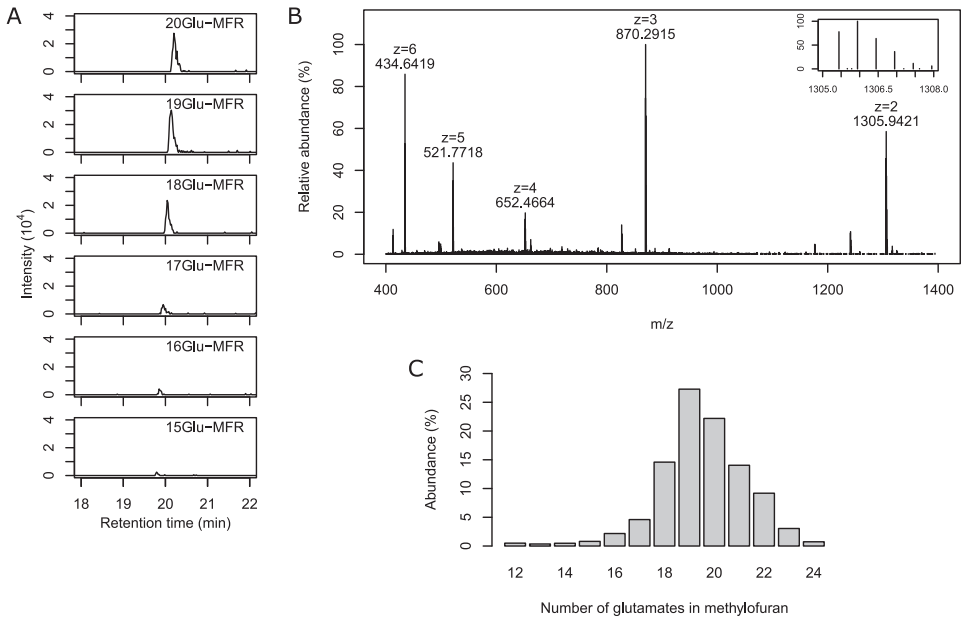

FIGURE 4. **Analysis of methylofuran by nano-ion-pair reversed-phase LC-MS.** *A*, extracted ion chromatograms of six different species of methylofuran with different numbers of glutamic acid residues in the side chain, shown as the sum of the charge states with $2 \leq z \leq 9$. *B*, mass spectrum showing some of the different charge states of the $[M\text{-}zH]^{z-}$ ions generated during negative ionization of methylofuran, shown here for the example of methylofuran containing 18 glutamic acids. The *inset* displays a zoomed-in view showing the natural abundance isotope pattern of the $z = 2$ peak. *C*, distribution of the number of glutamic acid residues in the side chain of the different species of methylofuran. The distribution was calculated by integration of the intensity of all charge states and all natural isotopologues for each species.

in the order of increasing number of glutamic acid residues (Fig. 4*A*). Because of the acidity of the glutamic acids, the MFR species were present in different charge states with $2 \leq z \leq 9$ in the (negative ion) mass spectrum (Fig. 4*B*). The retention time and charge states of methylofuran were very similar to those of the $(\gamma E)_{20}Y$ polyglutamic acid standard, indicating a similar chemical structure.

From the intensity of the ions corresponding to the different species of methylofuran, a distribution showing the abundance of each species was calculated (Fig. 4*C*). The distribution might, however, be affected by different ionization efficiencies for the different species, although this influence was assumed to be small, especially for species differing only by a small number of glutamic acids. The distribution was roughly normal and showed the presence of methylofuran species with 12 up to 24 glutamic acid residues in their side chain. The most abundant methylofuran species contained 19 glutamic acids and made up almost a third of all the species, although the center of the distribution showed some batch-to-batch variation (±1 glutamic acid).

Based on the exact masses of methylofurans (Table 1) and assuming a core structure linked to unmodified glutamic acids, we could determine the molecular formula to be $C_{15}H_{18}N_2O_4 + nC_5H_7NO_3$, with n ranging from 12 to 24, thus with a molecular mass of up to 3387.15 Da. The molecular formula assigned to the core structure differs from the APMF core structure present in all known methanofurans ($C_{14}H_{18}N_2O_2$) (22) by CO_2, indicating an additional functional group(s) attached to its core structure, *e.g.* in the form of a carboxylic acid group.

For the further structural characterization of methylofuran, LC-MS-MS analysis was carried out. For the general characterization of the fragmentation pattern of methylofuran, analysis was performed with methylofuran containing 20 and 19 glutamic acid residues. The fragmentation of both methylofurans resulted in two distinct series of fragments separated by the mass of a glutamic acid residue (Fig. 5). One series corresponded to the loss of single glutamic acids from the side chain of methylofuran, still containing the core structure (Table 2). The other series was due to the loss of the core structure together with various numbers of glutamic acid residues, thereby generating a series of polyglutamic acids of various lengths (Table 2). Additionally, one or multiple water losses was commonly observed in both series. The observed fragmentation pattern was similar to the MS-MS analysis of the $(\gamma E)_{20}Y$ peptide standard, where the same two series of fragments were observed (Table 2). Because polyglutamic acid fragments with up to 19 residues were observed for methylofuran containing 20 glutamic acids, any modification of the glutamic acids in the side chain is very unlikely. Most importantly, a fragment corresponding to the core structure of methylofuran without any glutamic acids was also detected (Table 2). Its mass differed from APMF by the mass of CO_2, and the calculated mass of the neutral loss corresponded to an unmodified polyglutamic acid chain of 20 residues, which confirmed the modification being located in the core structure.

Peaks matching the mass of the formylated form of methylofuran (structure in Fig. 2*C*) and eluting ~25 s later than their non-formylated counterparts were also identified, although with much lower intensity (data not shown). One reason for the predominance of the non-formylated forms of methylofuran might be the fast hydrolysis of the formyl group to formate, which is catalyzed by the same enzyme complex (FhcABCD) as the formyl transfer from H_4MPT to methylofuran (15).

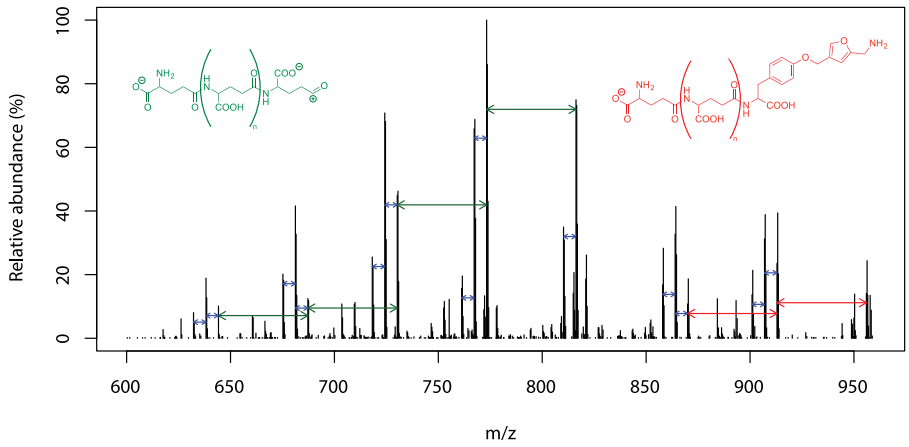

FIGURE 5. **MS-MS fragmentation spectrum of methylofuran.** The spectrum shows a zoomed-in view of the fragmentation pattern for the fragmentation of the $[M-3H]^{3-}$ parent ion of methylofuran containing 20 glutamic acid residues (955.98 *m/z*). The *long arrows* (*green* and *red*) correspond to losses of glutamic acid (43.0142 *m/z* for $z = 3$), whereas the *short arrows* (*blue*) correspond to water losses (6.0035 *m/z* for $z = 3$). The peaks separated by *green arrows* emerge from the polyglutamic acid molecule drawn in *green* (generated through the loss of the core structure from methylofuran), whereas the peaks separated by *red arrows* arise from simple glutamic acid losses of methylofuran.

TABLE 2

List of the MS-MS fragments obtained during fragmentation of methylofuran and the $(\gamma E)_{20}Y$ peptide standard

Selected fragment ions of the $[M-3H]^{3-}$ parent ion of methylofurans containing 20 and 19 glutamic acid residues (955.98 *m/z*, 912.97 *m/z*). For comparison, only the corresponding fragments of the $(\gamma E)_{20}Y$ peptide standard (919.64 *m/z*) are shown, although the whole series of Glu_n-core and Glu_n fragments with $1 \leq n \leq 20$ was observed (with the exception of Glu_{19} and Glu_{18}). "core" indicates the identified core structure of methylofuran ($C_{15}H_{18}N_2O_4$) or a tyrosine residue in the case of the peptide standard. *m/z* values for the observed (multiple) water losses are also not listed. NM, not measured, ND, not detected.

	Measured *m/z*			
Fragment	Glu_{20}-MFR	Glu_{19}-MFR	γGlu_{20} Tyr peptide	*z*
Glu_{20}-core	955.9847		919.6417	3
Glu_{19}-core	912.9704	912.9711	876.6187	3
Glu_{18}-core	869.9576	869.9567	833.6081	3
Glu_{17}-core	826.9415	826.9434	790.5964	3
Glu_{16}-core	783.9303	783.9265	747.5732	3
Glu_1-core	418.1619	418.1617	309.1091	1
Core	289.1192	289.1190	NM	1
Glu_{20}	ND		1289.4187	2
Glu_{19}	816.2625	ND	ND	3
Glu_{18}	773.2481	773.2484	ND	3
	1160.3754	1160.3770	1160.3747	2
Glu_{17}	1095.8535	1095.8532	1095.8543	2
Glu_{16}	687.2207	687.2192	1031.3334 ($z = 2$)	3
Glu_{15}	644.2055	644.2055	966.8093 ($z = 2$)	3
Glu_4	515.1628	515.1628	515.1631	2
Glu_3	386.1205	386.1203	386.1204	3
Glu_2	257.0774	257.0775	257.0777	3
Glu_1	128.0338	NM	NM	1

TABLE 3

NMR chemical shifts of methylofuran

Chemical shifts were measured in D_2O at 298 K and referenced with DSS. Annotation of the protons is according to Fig. 2*B*.

Poly-Glu side chain protons	$\delta\ ^1H_{(DSS)}$
α-Linked-Glu	*ppm*
H_α	4.07
H_β and $H_{\beta'}$	1.78–1.93 (broad)
H_γ	2.16–2.29 (broad)
γ-Linked-Glu	
H_α	3.96
H_β	1.78–1.93 (broad)
$H_{\beta'}$	1.75–1.63 (broad)
H_γ	1.63–1.75
Core structure protons	**$\delta\ ^1H_{(DSS)}$**
Tyrosine moiety	*ppm*
H_α	4.23
H_β	2.99
$H_{\beta'}$	2.67
H_δ	7.01
H_ϵ	6.78
Furan moiety	
H_1	4.05
H_3	6.49
H_5	7.49
H_6	4.81

In a culture grown on succinate instead of methanol, methylofuran could also be detected and was present in similar quantities. Thus, methylofuran was produced even though no one-carbon substrate was present, an observation that is in-line with the detection of the converting enzymes under non-methylotrophic growth conditions (7, 34, 35).

Determination of the Core Structure of Methylofuran—From the MS data, it is evident that the core structure of methylofuran contained an additional modification corresponding to the atoms CO_2 compared with the APMF core structure. The simplest form of such a modification would be a carboxylic acid group. From the initial NMR data (see above), it was concluded that the furan ring and the tyramine-like aromatic ring are unmodified compared with known MFRs because resonances for all the protons were detected. Therefore, the only four possible positions left for a modification in the APMF core structure were: the two methylene groups attached to the furan moiety and the two methylene groups in the tyramine-like moiety. The two methylene groups attached to the furan ring in the α position of the amine and in the α position of the phenoxy group were assigned at 4.05 ppm and 4.81 ppm, respectively (Table 3). These chemical shifts exclude any carboxylation, as 4.81 ppm is similar to the chemical shift found for formyl-MFR-a (4.84 ppm), and 4.05 ppm is at higher field compared with the 4.26 ppm determined for formyl-MFR-a and compared with the expected chemical shift of the H_α of α amino acids (*i.e.* above 5.0 ppm). Considering the two methylene groups in the tyramine-like moiety, the position next to the amine group was considered more likely to be modified, as the attachment of a carboxylic acid group at that position would result in a tyrosine residue instead of a tyramine. Furthermore,

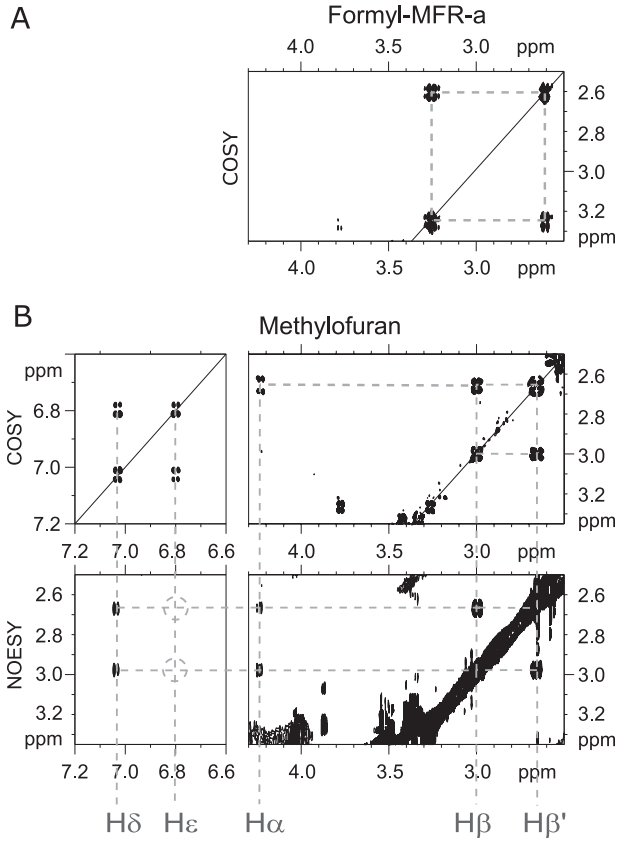

FIGURE 6. **Structural elucidation of the tyrosine moiety in the core structure of methylofuran.** Peaks are annotated according to Fig. 2*B*. Spectra were recorded at 298 K in D_2O and calibrated with respect to 4,4-dimethyl-4-silapentane-1-sulfonic acid (DSS). *A*, part of the $^1H,^1H$ COSY spectrum of formyl-MFR-a, showing the connectivity of the two methylene groups of the tyramine moiety. *B*, part of the $^1H,^1H$ COSY (*top panel*) and $^1H,^1H$ NOESY (*bottom panel*) spectrum of methylofuran, illustrating the complete connectivity of the tyrosine spin system, which is present in methylofuran instead of the tyramine moiety in MFR-a.

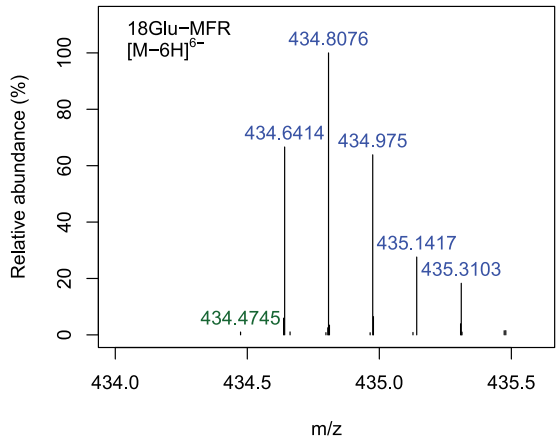

FIGURE 7. **Mass spectrum of methylofuran containing a ^{13}C-labeled carboxylic acid group in the tyrosine residue.** The spectrum shows the natural abundance isotope pattern of the $[M-6H]^{6-}$ ion of the labeled methylofuran containing 18 glutamic acid residues (*blue peaks*). The *green peak* corresponds to a minor amount of unlabeled species still being present. The shift between the green and the first blue peak (monoisotopic peak) corresponds to the mass difference between a ^{13}C and a ^{12}C atom (0.1672 *m/z* for $z = 6$).

in the biosynthesis of the methanogenic MFR, the tyramine residue is formed by the decarboxylation of tyrosine (23). In methylofuran, a tyrosine residue instead of a tyramine could, therefore, easily be explained by a modified biosynthesis where the decarboxylation step is missing. To prove this hypothesis, NMR and *in vivo* ^{13}C labeling of the tyrosine moiety were applied.

Comparison of the COSY spectrum of formyl-MFR-a (Fig. 6*A*) with the spectrum of methylofuran (Fig. 6*B*, *top panel*) clearly demonstrates that the spin system assigned to the α and β methylene groups of the tyramine moiety (*i.e.* 3.26 and 2.61 ppm, respectively) is absent in the COSY spectrum of methylofuran, suggesting a structural modification in this region of the molecule. In contrast, the COSY spectrum of methylofuran reveals a unique spin system at 4.23, 2.99, and 2.67 ppm, which is within the range of the chemical shifts given in the literature (Biological Magnetic Resonance Data Bank) for a tyrosine residue (4.61 ± 0.6 ppm for H_α and 2.89 ± 0.5 and 2.83 ± 0.5 ppm for H_β) and in line with a carboxylation at the level of the methylene at the α position of the tyramine moiety. The NOESY spectrum (Fig. 6*B*, *bottom panel*) displays cross-peaks between the two protons of the tyrosine methylene group (H_β) and the two protons at the δ position in the aromatic ring, confirming the presence of a tyrosine moiety instead of a tyramine in methylofuran in *M. extorquens* AM1 (Fig. 2*B*).

For the further validation of the presence of a non-decarboxylated tyrosine residue in methylofuran, *in vivo* incorporation of ^{13}C-labeled tyrosine was performed through the addition of labeled tyrosine to the growth medium. The ability of *M. extorquens* to take up tyrosine from the medium has previously been reported (36). In a first step, tyrosine labeled with ^{13}C at the carbonyl position was used. After extraction and purification, the labeled methylofuran was analyzed by LC-MS. In the mass spectrum, a shift of one mass unit was observed, thereby proving the presence of the carboxylic acid group (Fig. 7). The unlabeled peak was only marginally visible, and the labeling efficiency was >98%.

In addition, a labeling experiment with completely ^{13}C- and ^{15}N-labeled tyrosine was performed to show that the tyrosine is incorporated as a whole and without any modification of the carbon atoms. In the resulting mass spectrum, peaks corresponding to the fully labeled tyrosine were observed (data not shown). Additionally, a peak shifted by only 9 instead of 10 mass units was observed. This peak was most likely due to the exchange of the amine ^{15}N through ^{14}N by the activity of transaminases (36). Together, both experiments show that tyrosine is incorporated into methylofuran without decarboxylation and without any further modification of the carbon backbone.

Discussion

In this work we demonstrate the presence of methylofuran, which is involved in methylotrophy, in *M. extorquens* AM1. Our structural characterization of the one-carbon carrier by means of mass spectrometry and NMR revealed a modified core structure compared with known archaeal MFRs that share the same APMF core structure. Instead of the tyramine residue usually present in the core structure, methylofuran contains a non-decarboxylated tyrosine residue. This modification leads to a simplified biosynthesis of methylofuran, as the tyrosine molecule can be incorporated directly, thus obviating the need for the L-tyrosine

decarboxylase (MfnA) used in the archaeal MFR biosynthesis (23). The circumvention of decarboxylation is further supported by a BLASTP search (37) that revealed the absence of an MfnA ortholog in *M. extorquens* AM1. An open question is the biochemical significance of the additional carboxylic acid group and whether it is required in *M. extorquens* for the recognition and activity of the cofactor *in vivo*; conversely, it is also not known whether MfnA is dispensable in methanogenic archaea.

Another difference between the methylofuran in *M. extorquens* and other known MFRs is the larger number of glutamic acids in the side chain of methylofuran. The largest MFR known until now, MFR-d, contains 7–12 glutamic acid residues (22), whereas we have identified between 12 and 24 residues for methylofuran. Methylofuran is, therefore, to our knowledge the largest cofactor described so far.

In addition to containing a larger number of glutamic acids, methylofuran also shows a broader distribution of the different species. This finding raises interesting questions regarding the biological reason for the broad distribution and the large number of glutamic acid residues. The distribution might be stochastic as a result of an imperfect biosynthesis, although it might also play a role in regulation, as the large number of glutamic acids might affect the binding and recognition of the cofactor by the involved enzymes.

The last striking difference between the methylofuran from *M. extorquens* AM1 and the other known MFRs concerns the type of linkage between the glutamic acid residues. Although the other known MFRs contain exclusively γ-linked glutamic acids, we detected both α- and γ-linkages. It is currently unknown which enzyme is involved in the formation of the peptide bonds and whether side-chain elongation proceeds progressively from the core structure or is transferred en bloc.

Taken together, we here identified the methylofuran from *M. extorquens* AM1, which differs from the MFRs in methanogenic archaea described thus far. It will be interesting to also identify methylofurans in other aerobic methylotrophic bacteria found to contain H_4MPT/methylofuran-dependent enzymes (10, 38) and to analyze the structure of the methylofuran(s) in light of the Fhc that apparently lost formyl-MFR dehydrogenase activity found in methanogenic archaea (15).

Author Contributions—J. L. H. and B. K. S. purified methylofuran. J. L. H., A. M. O., and P. K. conducted LC-MS experiments and analyzed the data. O. S. performed the NMR measurements. O. S. and A. M. analyzed the NMR data. J. A. V. initiated and supervised the research. All authors discussed the research and contributed to writing the manuscript.

Acknowledgments—We thank Philipp Christen, ETH Zurich, for support in running fed-batch cultures. The IPBS (Institute of Pharmacology and Structural Biology) NMR equipment belonged to the Genotoul-PICT platform and received specific funding by Ibisa, the Région Midi-Pyrénées and European structural funds.

References

1. Leigh, J. A., and Wolfe, R. S. (1983) Carbon dioxide reduction factor and methanopterin, two coenzymes required for CO_2 reduction to methane by extracts of *Methanobacterium*. *J. Biol. Chem.* **258,** 7536–7540
2. Leigh, J. A., Rinehart, K. L., and Wolfe, R. S. (1984) Structure of methanofuran, the carbon dioxide reduction factor of *Methanobacterium thermoautotrophicum*. *J. Am. Chem. Soc.* **106,** 3636–3640
3. Keltjens, J. T., Huberts, M. J., Laarhoven, W. H., and Vogels, G. D. (1983) Structural elements of methanopterin, a novel pterin. *Eur. J. Biochem.* **130,** 537–544
4. Escalante-Semerena, J. C., Rinehart, K. L., Jr., and Wolfe, R. S. (1984) Tetrahydromethanopterin, a carbon carrier in methanogenesis. *J. Biol. Chem.* **259,** 9447–9455
5. Taylor, C. D., and Wolfe, R. S. (1974) Structure and methylation of coenzyme M ($HSCH_2CH_2SO_3$). *J. Biol. Chem.* **249,** 4879–4885
6. DiMarco, A. A., Bobik, T. A., and Wolfe, R. S. (1990) Unusual coenzymes of methanogenesis. *Annu. Rev. Biochem.* **59,** 355–394
7. Chistoserdova, L., Vorholt, J. A., Thauer, R. K., and Lidstrom, M. E. (1998) C1 transfer enzymes and coenzymes linking methylotrophic bacteria and methanogenic archaea. *Science* **281,** 99–102
8. Pomper, B. K., Vorholt, J. A., Chistoserdova, L., Lidstrom, M. E., and Thauer, R. K. (1999) A methenyl tetrahydromethanopterin cyclohydrolase and a methenyl tetrahydrofolate cyclohydrolase in *Methylobacterium extorquens* AM1. *Eur. J. Biochem.* **261,** 475–480
9. Chistoserdova, L., Vorholt, J. A., and Lidstrom, M. E. (2005) A genomic view of methane oxidation by aerobic bacteria and anaerobic archaea. *Genome Biol.* **6,** 208
10. Chistoserdova, L., Jenkins, C., Kalyuzhnaya, M. G., Marx, C. J., Lapidus, A., Vorholt, J. A., Staley, J. T., and Lidstrom, M. E. (2004) The enigmatic planctomycetes may hold a key to the origins of methanogenesis and methylotrophy. *Mol. Biol. Evol.* **21,** 1234–1241
11. Vorholt, J. (2002) Cofactor-dependent pathways of formaldehyde oxidation in methylotrophic bacteria. *Arch. Microbiol.* **178,** 239–249
12. Vorholt, J. A., Marx, C. J., Lidstrom, M. E., and Thauer, R. K. (2000) Novel formaldehyde-activating enzyme in *Methylobacterium extorquens* AM1 required for growth on methanol. *J. Bacteriol.* **182,** 6645–6650
13. Hagemeier, C. H., Chistoserdova, L., Lidstrom, M. E., Thauer, R. K., and Vorholt, J. A. (2000) Characterization of a second methylene tetrahydromethanopterin dehydrogenase from *Methylobacterium extorquens* AM1. *Eur. J. Biochem.* **267,** 3762–3769
14. Pomper, B. K., and Vorholt, J. A. (2001) Characterization of the formyltransferase from *Methylobacterium extorquens* AM1. *Eur. J. Biochem.* **268,** 4769–4775
15. Pomper, B. K., Saurel, O., Milon, A., and Vorholt, J. A. (2002) Generation of formate by the formyltransferase/hydrolase complex (Fhc) from *Methylobacterium extorquens* AM1. *FEBS Lett.* **523,** 133–137
16. Chistoserdova, L., Laukel, M., Portais, J.-C., Vorholt, J. A., and Lidstrom, M. E. (2004) Multiple formate dehydrogenase enzymes in the facultative methylotroph *Methylobacterium extorquens* AM1 are dispensable for growth on methanol. *J. Bacteriol.* **186,** 22–28
17. Anthony, C. (1982) *The Biochemistry of Methylotrophs*, pp. 95–136, Academic Press, London
18. Large, P., Peel, D., and Quayle, J. (1961) Microbial growth on C1 compounds. 2. Synthesis of cell constituents by methanol- and formate-grown *Pseudomonas* AM 1, and methanol-grown *Hyphomicrobium vulgare*. *Biochem. J.* **81,** 470–480
19. Marx, C. J., Laukel, M., Vorholt, J. A., and Lidstrom, M. E. (2003) Purification of the formate-tetrahydrofolate ligase from *Methylobacterium extorquens* AM1 and demonstration of its requirement for methylotrophic growth. *J. Bacteriol.* **185,** 7169–7175
20. Bobik, T. A., Donnelly, M. I., Rinehart, K. L., Jr., and Wolfe, R. S. (1987) Structure of a methanofuran derivative found in cell extracts of *Methanosarcina barkeri*. *Arch. Biochem. Biophys.* **254,** 430–436
21. White, R. H. (1988) Structural diversity among methanofurans from different methanogenic bacteria. *J. Bacteriol.* **170,** 4594–4597
22. Allen, K. D., and White, R. H. (2014) Identification of structurally diverse methanofuran coenzymes in *Methanococcales* that are both *N*-formylated and *N*-acetylated. *Biochemistry* **53,** 6199–6210
23. Kezmarsky, N. D., Xu, H., Graham, D. E., and White, R. H. (2005) Identification and characterization of a L-tyrosine decarboxylase in *Methanocaldococcus jannaschii*. *Biochim. Biophys. Acta* **1722,** 175–182
24. Miller, D., Wang, Y., Xu, H., Harich, K., and White, R. H. (2014) Biosyn-

thesis of the 5-(aminomethyl)-3-furanmethanol moiety of methanofuran. *Biochemistry* **53,** 4635–4647
25. Wang, Y., Xu, H., Harich, K. C., and White, R. H. (2014) Identification and characterization of a tyramine-glutamate ligase (Mfnd) involved in methanofuran biosynthesis. *Biochemistry* **53,** 6220–6230
26. Wang, Y., Xu, H., Jones, M. K., and White, R. H. (2015) Identification of the final two genes functioning in methanofuran biosynthesis in *Methanocaldococcus jannaschii*. *J. Bacteriol.* **197,** 2850–2858
27. Shima, S., and Thauer, R. K. (2001) Tetrahydromethanopterin-specific enzymes from *Methanopyrus kandleri*. *Methods enzymol.* **331,** 317–353
28. Liu, M., Mao, X.-a., Ye, C., Huang, H., Nicholson, J. K., and Lindon, J. C. (1998) Improved watergate pulse sequences for solvent suppression in NMR spectroscopy. *J. Magn. Reson.* **132,** 125–129
29. Derome, A. E., and Williamson, M. P. (1990) Rapid-pulsing artifacts in double-quantum-filtered COSY. *J. Magn. Reson.* **88,** 177–185
30. Bax, A., and Davis, D. G. (1985) MLEV-17-based two-dimensional homonuclear magnetization transfer spectroscopy. *J. Magn. Reson.* **65,** 355–360
31. Kiefer, P., Delmotte, N., and Vorholt, J. A. (2011) Nanoscale ion-pair reversed-phase HPLC-MS for sensitive metabolome analysis. *Anal. Chem.* **83,** 850–855
32. Kiefer, P., Schmitt, U., and Vorholt, J. A. (2013) Emzed: An open source framework in python for rapid and interactive development of LC/MS data analysis workflows. *Bioinformatics* **29,** 963–964
33. Kasai, T., and Sakamura, S. (1973) Distinction between α- and γ-glutamyl dipeptides by means of NMR spectrometer and amino acid analyzer. *Agric. Biol. Chem.* **37,** 685–686
34. Laukel, M., Rossignol, M., Borderies, G., Völker, U., and Vorholt, J. A. (2004) Comparison of the proteome of *Methylobacterium extorquens* AM1 grown under methylotrophic and nonmethylotrophic conditions. *Proteomics* **4,** 1247–1264
35. Bosch, G., Skovran, E., Xia, Q., Wang, T., Taub, F., Miller, J. A., Lidstrom, M. E., and Hackett, M. (2008) Comprehensive proteomics of *Methylobacterium extorquens* AM1 metabolism under single carbon and nonmethylotrophic conditions. *Proteomics* **8,** 3494–3505
36. Houck, D. R., Hanners, J. L., and Unkefer, C. J. (1991) Biosynthesis of pyrroloquinoline quinone. 2. Biosynthetic assembly from glutamate and tyrosine. *J. Am. Chem. Soc.* **113,** 3162–3166
37. Altschul, S. F., Madden, T. L., Schäffer, A. A., Zhang, J., Zhang, Z., Miller, W., and Lipman, D. J. (1997) Gapped BLAST and PSI-BLAST: a new generation of protein database search programs. *Nucleic Acids Res.* **25,** 3389–3402
38. Vorholt, J. A., Chistoserdova, L., Stolyar, S. M., Thauer, R. K., and Lidstrom, M. E. (1999) Distribution of tetrahydromethanopterin-dependent enzymes in methylotrophic bacteria and phylogeny of methenyl tetrahydromethanopterin cyclohydrolases. *J. Bacteriol.* **181,** 5750–5757

The One-carbon Carrier Methylofuran from *Methylobacterium extorquens* AM1 Contains a Large Number of α- and γ-Linked Glutamic Acid Residues

Jethro L. Hemmann, Olivier Saurel, Andrea M. Ochsner, Barbara K. Stodden, Patrick Kiefer, Alain Milon and Julia A. Vorholt

J. Biol. Chem. 2016, 291:9042-9051.
doi: 10.1074/jbc.M116.714741 originally published online February 19, 2016